Electronic Supplementary Material (ESI) for Journal of Materials Chemistry C.

Supplementary information for:

Role of excess tellurium on the electrical and thermal properties in Te-doped paracostibite

G. Guélou[1], F. Failamani[1], P. Sauerschnig[1], J. Waybright[1], K. Suzuta[1] and T. Mori[1,2]

An initial Te-substituted paracostibite series was produced to confirm the optimum substitution level of 4% established by Chmielowski *et al.*,[1] following the procedure described in the article. All XRD data were acquired on the samples after SPS and annealing and Rietveld refinements were carried out, Fig. S1, confirming the variation of the unit cell parameters across the series to follow Vegard's law, Fig. S7. The samples are mostly pure with traces amounts of an identified second phase. We see from the evolution of the thermoelectric properties, Fig. S2, that we do observe an optimum doping level of 4%, although our $CoSb_{0.96}Te_{0.04}S$ (ZT ≈ 0.25 at 773 K) was not as performing as the previously reported ZT of 0.47 at 725 K. We have not been able to clearly identify the reason behind these discrepancies, however, we did use longer synthesis times and a higher sintering temperature. In our case, such SPS conditions were necessary to achieve satisfactory densification (>95% of crystallographic value) and robustness. Attempts to consolidate paracostibite at a lower temperature yielded very brittle samples. This was particularly important as we then induced porosity and needed a sufficiently high temperature to liquefy the second phase. As seen from Fig. S3, the displacement of the plunger during sintering relative to the temperature is characteristic of optimal conditions. Moreover, we see from the sintering of $CoSb_{0.96}Te_{0.04}S[Te]_{0.28}$ that 650°C is the required temperature to insure both optimal sintering and the removal of the second phase.

From the above observations, we can assume that more "classic" tellurium substitution for antimony does not lead to further improvement in ZT. Because of the synthesis and SPS conditions, we can speculate that our samples may contain a higher concentration of electron killing defects such as S_{Sb}.[1,2]

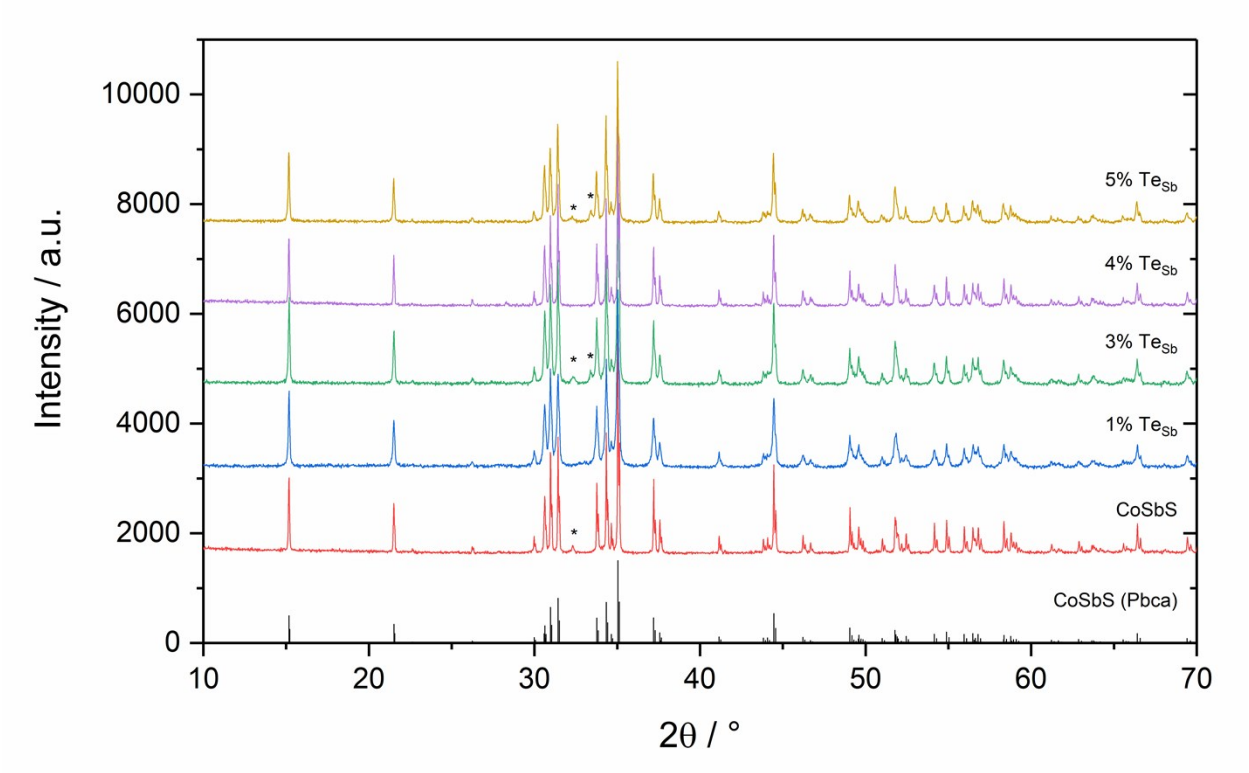

Fig. S1 X-ray diffraction patterns for $CoSb_{1-x}Te_xS$ (x = 0, 0.01, 0.03, 0.04, 0.05).

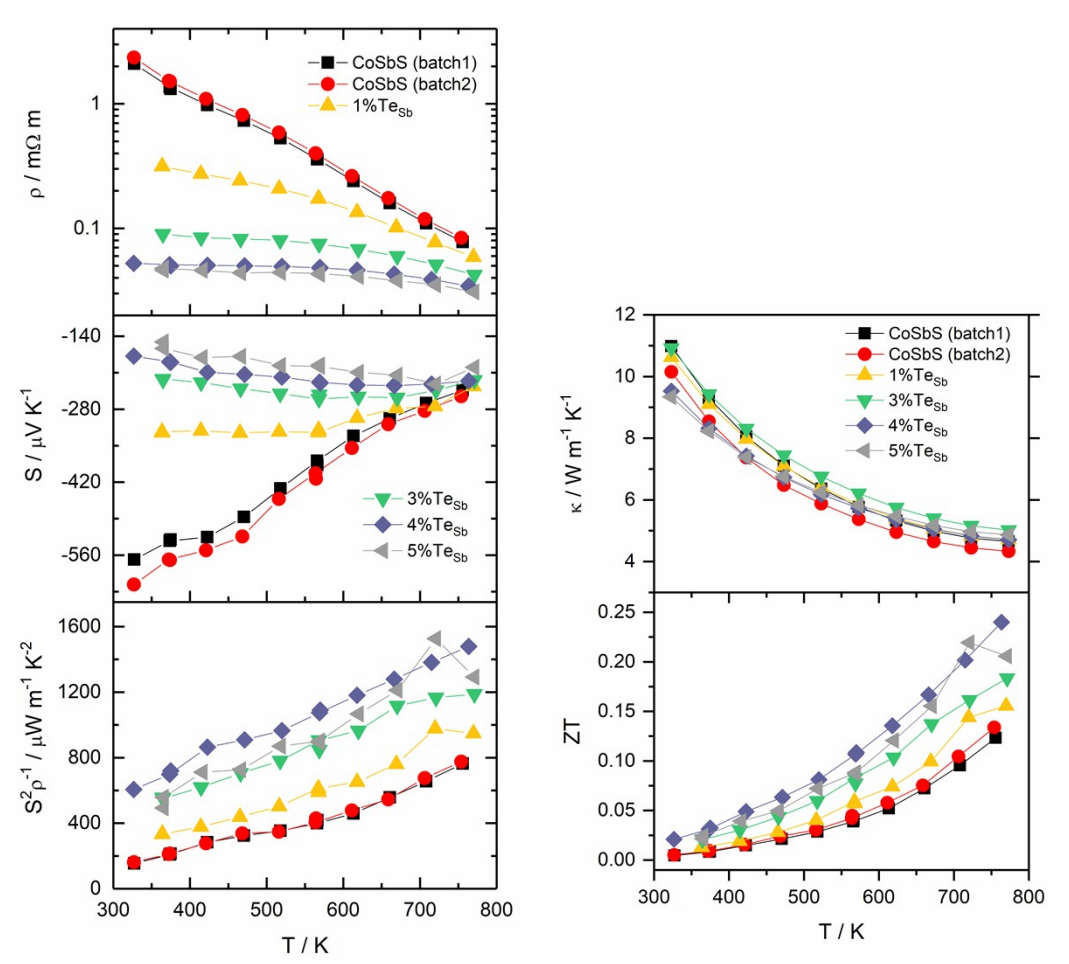

Fig. S2 Temperature dependence of the electrical resistivity, Seebeck coefficient, power factor, thermal conductivity and ZT for $CoSb_{1-x}Te_xS$ (x = 0, 0.01, 0.03, 0.04, 0.05).

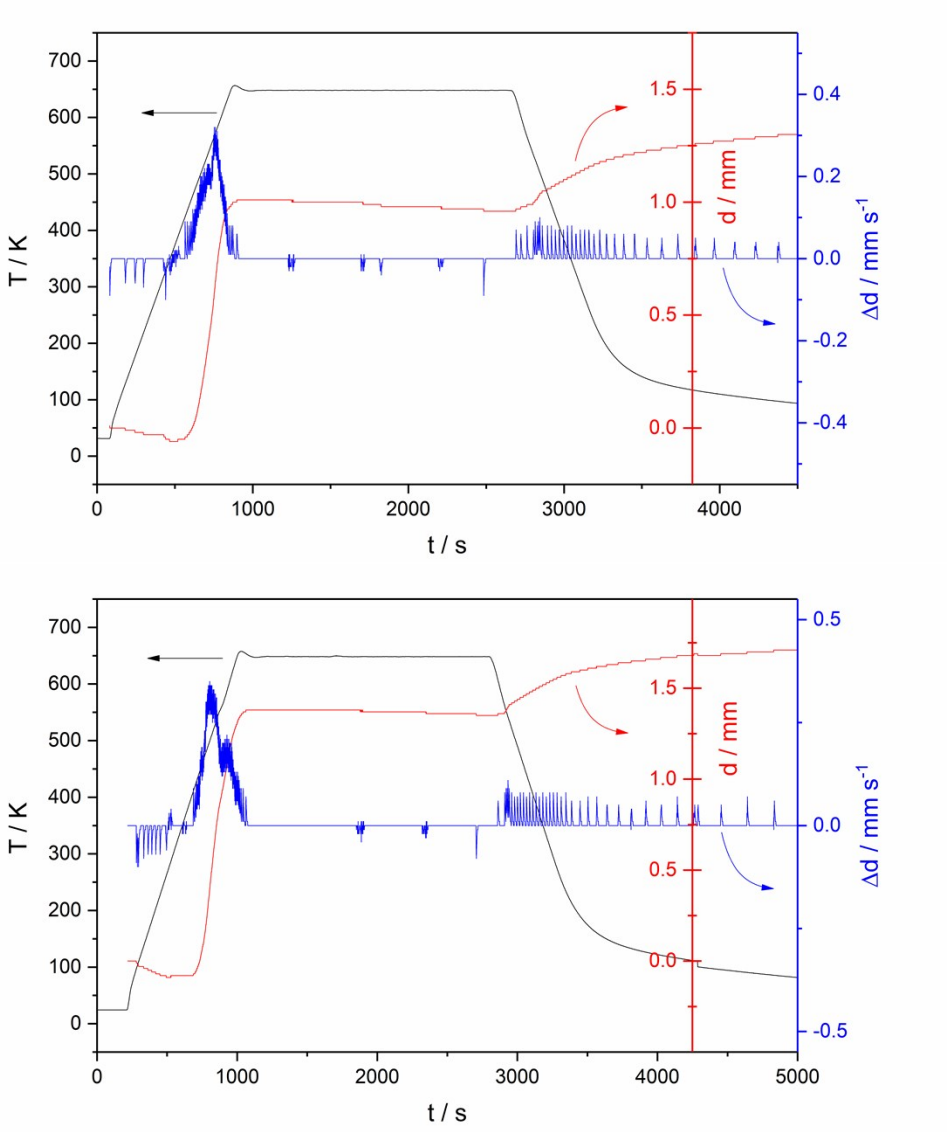

Fig. S3 The SPS profiles of $CoSb_{0.96}Te_{0.04}S$ (top) and $CoSb_{0.96}Te_{0.04}S[Te]_{0.28}$ (bottom).

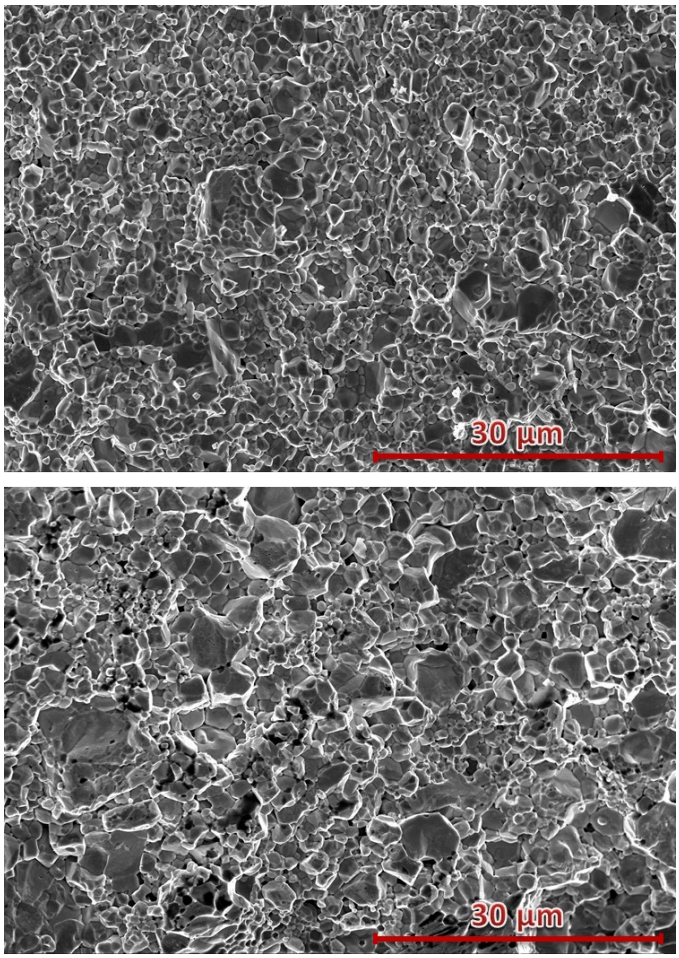

Fig. S4 Scanning electron micrographs of a fractured surface of $CoSb_{0.96}Te_{0.04}S$ (top) and $CoSb_{0.96}Te_{0.04}S[Te]_{0.28}$ (bottom) showing the differences in particle size distribution and concentration of pores.

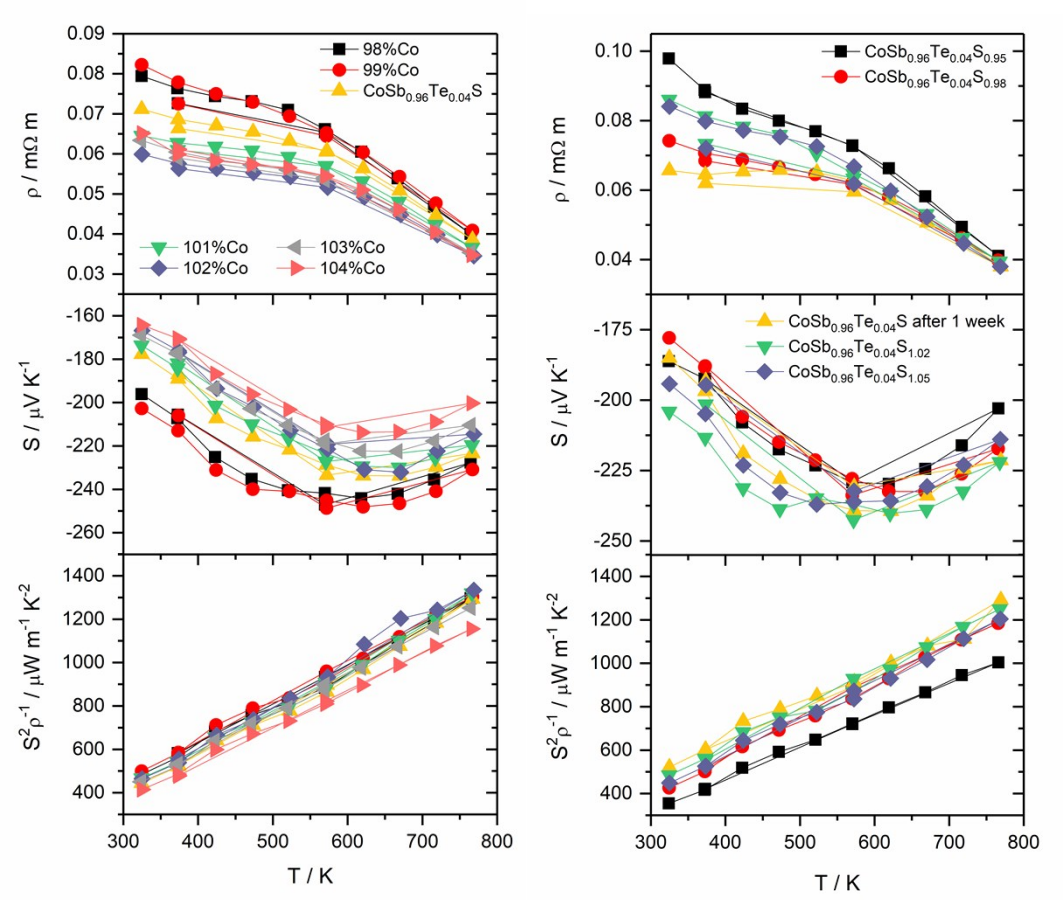

Fig. S5 Temperature dependence of the electrical resistivity, Seebeck coefficient and power factor for $Co_{1+x}Sb_{0.96}Te_{0.04}S$ (x = -0.02, -0.01, 0, 0.01, 0.02, 0.03, 0.04) and $CoSb_{0.96}Te_{0.04}S_{1+z}$ (z = -0.05, -0.02, 0, 0.02, 0.05). Data on cooling for all samples and data for $CoSb_{0.96}Te_{0.04}S$ after 1 week annealing at 923 K are also included.

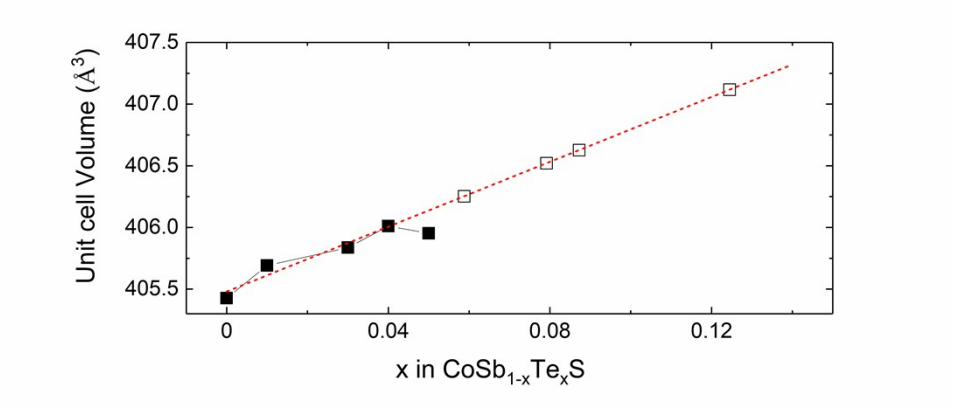

Fig. S6 Refined unit cell volume for $CoSb_{1-x}Te_xS$ (full symbols) and $CoSb_{0.96}Te_{0.04}S[Te]_y$ (open symbols). The value for x in $CoSb_{0.96}Te_{0.04}S[Te]_y$ was estimated from the dotted red linear tendency.

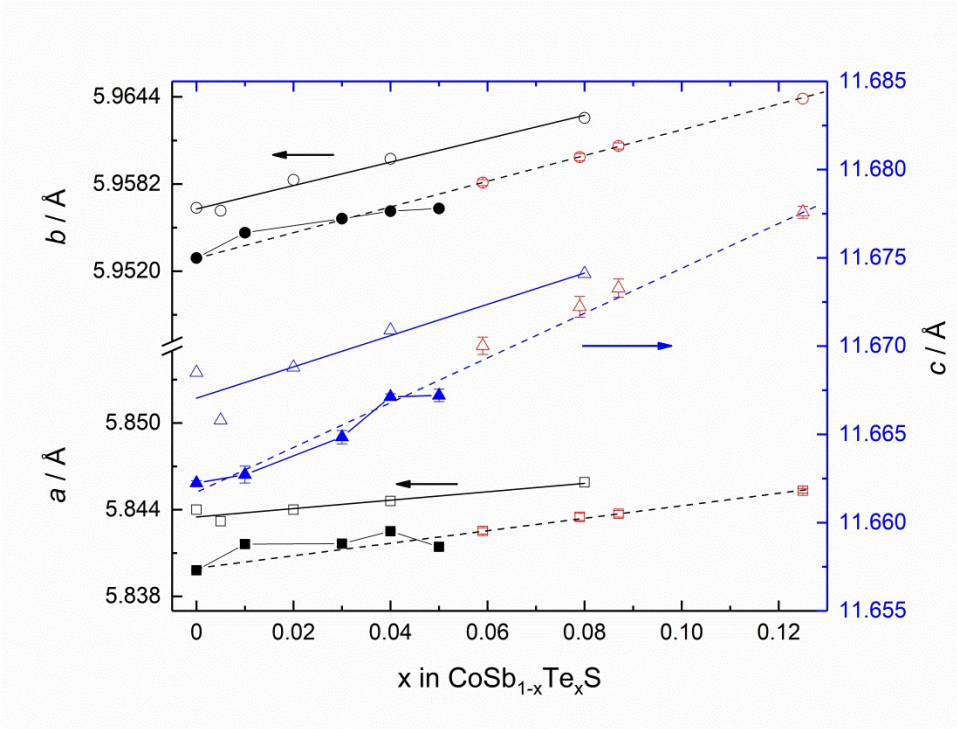

Fig. S7 Refined unit cell parameters for $CoSb_{1-x}Te_xS$ (full symbols) and $CoSb_{0.96}Te_{0.04}S[Te]_y$ (red open symbols) compared to data from the work of Chmielowski *et al*. (open symbols).[1]

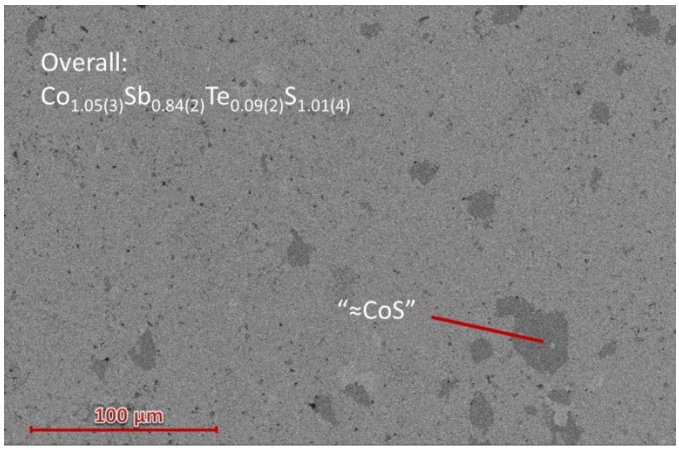

Fig. S8 Back-scattered electron (BSE) micrographs of polished surface of $CoSb_{0.96}Te_{0.04}S[Te]_{0.28}$ coupled with EDX analysis on a large surface (marked as overall) and on .

Table S1 Main phase composition of $CoSb_{0.96}Te_{0.04}S[Te]_x$ from WDX measurement.

Sample		Co	Sb	S	Te
x = 0.04	average	1.010	0.987	0.976	0.028
	min.	1.032	0.948	1.023	0.000
	max.	1.020	0.978	0.942	0.059
y = 0.07	average	0.983	1.025	0.947	0.046
	min.	0.993	1.023	0.945	0.040
	max.	0.981	1.020	0.945	0.056
y = 0.14	average	0.996	1.016	0.938	0.050
	min.	1.002	1.026	0.936	0.036
	max.	0.984	1.029	0.927	0.063
y = 0.21	average	0.987	1.019	0.936	0.057
	min.	0.981	1.026	0.960	0.032
	max.	1.002	0.999	0.927	0.073
y = 0.28	average	0.998	1.009	0.920	0.074
	min.	0.978	1.026	0.939	0.057
	max.	0.996	1.008	0.894	0.102

References

[1] R. Chmielowski, S. Bhattacharya, W. Xie, D. Péré, S. Jacob, R. Stern, K. Moriya, A. Weidenkaff, G. K. H. H. Madsen, G. Dennler, *J. Mater. Chem. C* **2016**, *4*, 3094.

[2] S. Bhattacharya, R. Chmielowski, G. Dennler, G. K. H. Madsen, *J. Mater. Chem. A* **2016**, *4*, 11086.